Lamellipodial localization of Dictyostelium myosin heavy chain kinase A is mediated via F-actin binding by the coiled-coil domain

By: Paul A. Steimle, Lucila Licate, Graham P. Côté, and Thomas T. Egelhoff

Edited by Amy McGough

Steimle, P.A., Licate, L., Côté, G.P., Egelhoff, T.T. (2002) Lamellipodial localization of *Dictyostelium* myosin heavy chain kinase A is mediated via F-actin binding by the coiled-coil domain. *FEBS Letters*. April 10, 516:58-62. doi:10.1016/S0014-5793(02)02494-8

:
Myosin heavy chain kinase A (MHCK A) modulates myosin II filament assembly in the amoeba *Dictyostelium discoideum*. MHCK A localization in vivo is dynamically regulated during chemotaxis, phagocytosis, and other polarized cell motility events, with preferential recruitment into anterior filamentous actin (F-actin)-rich structures. The current work reveals that an amino-terminal segment of MHCK A, previously identified as forming a coiled-coil, mediates anterior localization. MHCK A co-sediments with F-actin, and deletion of the amino-terminal domain eliminated actin binding. These results indicate that the anterior localization of MHCK A is mediated via direct binding to F-actin, and reveal the presence of an actin-binding function not previously detected by primary sequence evaluation of the coiled-coil domain.
Author Keywords: Myosin; Actin; Phosphorylation; Chemotaxis

Article:

1. Introduction

Myosin II displays polarized distribution in a variety of motile cell types, typically being depleted or absent in the leading edge and being present in increasing abundance towards the rear of the cell [1, 2 and 3]. This asymmetric accumulation of myosin II appears to be important for retraction of the cell posterior from the substratum, for generating translocation force with respect to the substratum, and may contribute to cortical retrograde cytoskeletal flow [4, 5 and 6].

Although myosin II has conserved roles in cytoskeletal organization, the mechanisms regulating myosin II localization and reorganization during dynamic processes such as chemotaxis are not well understood. In *Dictyostelium*, a family of related myosin heavy chain kinases (MHCKs) participate in myosin II filament assembly control by phosphorylating specific threonines in the tail region of MHC and driving filament disassembly [7, 8, 9 and 10]. The catalytic domain of MHCK A represents the founding example of a highly novel family of protein kinase catalytic domains, with several representatives in *Dictyostelium* [11, 12, 13 and 14], and a number of relatives in metazoan systems [15, 16 and 17].

MHCK A was recently reported to display dynamic recruitment to anterior filamentous actin (F-actin)-rich cellular protrusions. This behavior suggests a novel mechanism for spatial control of myosin II filament assembly, in which localized MHCK A accumulation may drive disassembly of myosin II filaments, preventing myosin II filament accumulation at sites of actin-based protrusive activity [18]. To address the mechanism responsible for MHCK A localization we have performed in vivo localization and in vitro actin-binding studies on point mutants and truncations of MHCK A. These studies demonstrate that the determinants for cortical recruitment and anterior localization reside within the amino-terminal coiled-coil domain of MHCK A. Biochemical analysis indicates that this segment of MHCK A also mediates direct F-actin binding in vitro.

These results suggest that direct binding of MHCK A to anterior F-actin in polarized cells is responsible for localization of MHCK A and subsequent localized inhibition of myosin II filament assembly.

2. Materials and methods

2.1. Plasmid constructs and cell lines

All green fluorescent protein (GFP)–MHCK A fusion constructs were based upon the expression vector pTX-GFP [19], which were transfected into a previously described MHCK A null cell line [10]. For chemoattractant response studies, cells were differentiated to the aggregation stage via cAMP pulsing and caffeine treatment as described previously [18].

The full-length GFP–MHCK A fusion contains an amino-terminal GFP domain fused to codon 2 of the MHCK A open reading frame, as described previously [18].

All amino acid residue numbering in this text refers to the GenBank entry for MHCK A (accession P42527). The GFP–C800A-MHCK A construct expresses an identical fusion product as the wild type full-length construct, except that cysteine residue 800 of MHCK A was converted to an alanine using PCR-based mutagenesis. The MHCK AΔWD construct is equivalent to the full-length MHCK A construct, except that gene truncation introduces a stop codon in the fusion protein after the isoleucine at position 842 of MHCK A. The MHCK A–WD construct expresses an amino-terminal GFP domain fused to the isolated WD repeat domain of MHCK A, including residues 844–1146. The MHCK AΔCoil construct contains an amino-terminal GFP domain fused to residues 499–1146 of MHCK A. The MHCK A–Coil construct expresses an amino-terminal GFP domain fused to residues 2–537 of MHCK A. GFP fusion constructs were introduced into an MHCK A null cell line via electroporation as described previously [20]. Truncation constructs used for F-actin-binding analysis contain amino-terminal 6×His tags rather than GFP tags, but fusion positions are similar to those of the GFP constructs. The construction of the His tag plasmids, and the purification of the expressed products from *Dictyostelium* cells has been described previously [21].

2.2. Immunoprecipitation and autophosphorylation

MHCK A null cells expressing either wild type MHCK A or the MHCK A–C800A construct were lysed in a buffer containing 50 mM TES, pH 7, 5 mM EDTA, 200 mM NaCl, and 1 mM dithiothreitol (DTT), with the addition of Triton X-100 to 1% final, in the presence of the protease inhibitor mixtures PIC I and PIC II [22]. GFP–MHCK A fusion proteins were immunoprecipitated by the addition of anti-GFP IgG (Molecular Probes) with a 30 min 4°C incubation, followed by the addition of protein-A-agarose beads (Boehringer Mannheim) with a 60 min 4°C incubation. Beads were collected by centrifugation and washed twice in 50 mM TES, 100 mM NaCl, 1 mM DTT, and 1 mM EDTA. A portion of the collected beads was subjected to Western blot analysis to confirm identity of the immunoprecipitated band (data not shown), and a portion of the beads was placed in kinase buffer (10 mM TES, pH 7, 2 mM $MgCl_2$, 2 mM ATP, 1 mM DTT) containing [^{32}P]γ-ATP to assess autophosphorylation activity. Samples were incubated for either 1 or 20 min, then heated in sample buffer and subjected to sodium dodecyl sulfate–polyacrylamide gel electrophoresis (SDS–PAGE). Following Coomassie staining and autoradiographic analysis, GFP–MHCK A bands were subjected to scintillation counting to quantify relative activity. In 1 min time point samples, ^{32}P incorporation was undetectable in the C800A-MHCK A construct (as shown in Fig. 1B). In 20 min time point samples, trace radioactivity was detected in the C800A-MHCK A band, but this was less than 0.5% of the level present in the wild type MHCK A band.

2.3. Microscopy

Approximately 2×10^5 of cAMP-pulsed, caffeine-treated cells were spotted on to a glass coverslip in a 100 μl volume and cells were allowed to adhere for at least 15 min. The cells were stimulated with 100 μM cAMP and images were collected at the times indicated with a Zeiss Axiovert microscope/LSM410 confocal laser system using an oil immersion Plan-Neofluor 100× objective lens (NA 1.3). Where indicated, cells were pre-treated for 15 min with 4 μM latrunculin A (Calbiochem).

2.4. Actin co-sedimentation assays

Rabbit skeletal muscle actin (Cytoskeleton, Denver, CO, USA) in 5 mM Tris–HCl, pH 8.0, 0.2 mM $CaCl_2$, 0.2 mM ATP, and 0.5 mM DTT was polymerized (30–60 min, 25°C) by the addition of 100 mM KCl, 2 mM $MgCl_2$, and 1 mM ATP from a concentrated stock. F-actin was incubated (1 h at 25°C) with 0.1 μM full-length MHCK A, Δ-WD MHCK A, or Δ-Coil MHCK A (as indicated) in a 40 μl reaction mix containing 12.5 mM Tris–HCl, pH 8.0, 0.1 mM $CaCl_2$, 5 mM EDTA, 0.5 mM DTT, 50 μg/ml bovine serum albumin (BSA), 175 μg/ml phenylmethylsulfonyl fluoride, and 2× concentration of protease inhibitor mixes PIC I and PIC II. Following incubation, reactions were spun for 30 min at 95 000×*g* and equal volumes of pellet and supernatant fractions were resolved by SDS–PAGE. Actin and BSA were visualized by Coomassie blue staining of gels. The distribution of MHCK A protein in pellets and supernatants was determined from Western blots probed with polyclonal anti-MHCK A antibody. The relative amounts of MHCK A protein in the pellet and supernatant fractions were quantified by densitometric analysis of the developed Western blots.

3. Results

MHCK A was originally identified as a biochemical activity capable of phosphorylating *Dictyostelium* myosin II and driving filament disassembly [23]. Subsequent cloning [12] and structure–function studies [11 and 21] revealed a domain organization consisting of an amino-terminal coiled-coil domain (~70 kDa) responsible for homo-oligomerization, a central catalytic domain (~25 kDa) completely unrelated to conventional protein kinases at the primary sequence level, and a carboxyl-terminal WD repeat domain (~35 kDa), as illustrated in Fig. 1A.

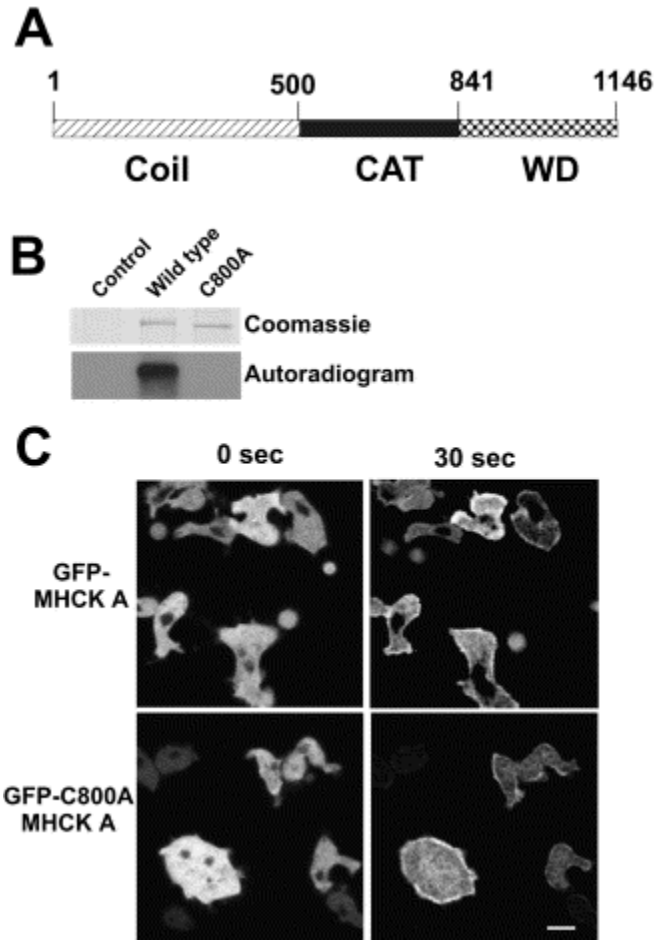

Fig. 1. A: Domain organization of MHCK A. B: GFP–C800A-MHCK A is deficient for autophosphorylation when isolated via immunoprecipitation. Anti-GFP antisera was used to perform immunoprecipitations from MHCK A null cells, or from cells expressing wild type or C800A MHCK A fused to GFP. Upper panel: Coomassie-stained immunoprecipitated GFP–MHCK A fusion protein from each cell line. Lower panel: Corresponding autoradiogram demonstrating loss of catalytic activity in the C800A mutant.

C: GFP–C800A-MHCK A displays normal recruitment to the cell cortex in response to chemoattractant stimulation. Confocal microscope images were collected before (0 s) or after (30 s) stimulation with the chemoattractant cAMP. Bar, 10 μM.

MHCK A translocates to the cell cortex in response to chemoattractant stimulation, and in polarized cells it displays preferential recruitment to anterior actin-rich structures such as lamellipodia and endocytic cups [18]. To determine whether kinase catalytic activity is required for chemoattractant-stimulated MHCK A translocation, we constructed a catalytically inactive derivative of MHCK A by converting a conserved cysteine at position 800 to an alanine. This residue is conserved in all identified members of this family of kinases [13 and 15], and in one mammalian family member, TRP-PLIK, mutations at this site were reported to eliminate catalytic activity [17]. We expressed and purified the catalytic domain of MHCK A bearing the C800A mutation in bacteria, and found no detectable catalytic activity with myelin basic protein or a peptide substrate (data not shown). When the C800A mutation was expressed in the context of GFP-tagged full-length MHCK A in a *Dictyostelium mhck*A null cell background, it also resulted in loss of kinase activity when assayed for autophosphorylation in immunoprecipitates (Fig. 1B).

As reported previously, full-length MHCK A fused to GFP translocated rapidly to the cell cortex upon chemoattractant stimulation (Fig. 1C, top panels). The kinase dead GFP–C800A-MHCK A fusion protein displayed robust translocation from the cytosol to the cell cortex upon stimulation (Fig. 1C, lower panels), indistinguishable from that observed for wild type MHCK A. This result indicates that chemoattractant-stimulated MHCK A translocation to the cell cortex does not depend upon kinase catalytic activity.

Given the earlier demonstration that the WD domains of MHCK A and B confer binding and enzymatic targeting to myosin II filaments [22], we conducted a series of truncation studies to determine if this domain of MHCK A also mediates translocation during chemoattractant responses. Deletion of the WD repeat domain did not impair chemoattractant-stimulated translocation of a GFP fusion protein to the cell cortex (Fig. 2, 'GFP–ΔWD'). A complementary construct, GFP fused to WD domain alone, displayed diffuse cytosolic localization even upon chemoattractant stimulation (Fig. 2, 'GFP–WD'). Deletion of the amino-terminal coiled-coil domain, however, resulted in a GFP fusion construct that lost the ability to translocate to the cell cortex upon stimulation (Fig. 2, 'GFP–ΔCoil'). The complementary construct fusing GFP to the coiled-coil domain alone displayed robust translocation upon stimulation (Fig. 2, 'GFP–Coil'). Consistent with earlier observations of full-length MHCK A [18], treatment of cells with latrunculin A to depolymerize F-actin resulted in a complete loss of translocation with this construct. These results indicate that the coiled-coil-containing domain of MHCK A is necessary and sufficient for cortical translocation in response to chemoattractant stimulation, and that cortical F-actin is necessary for this response.

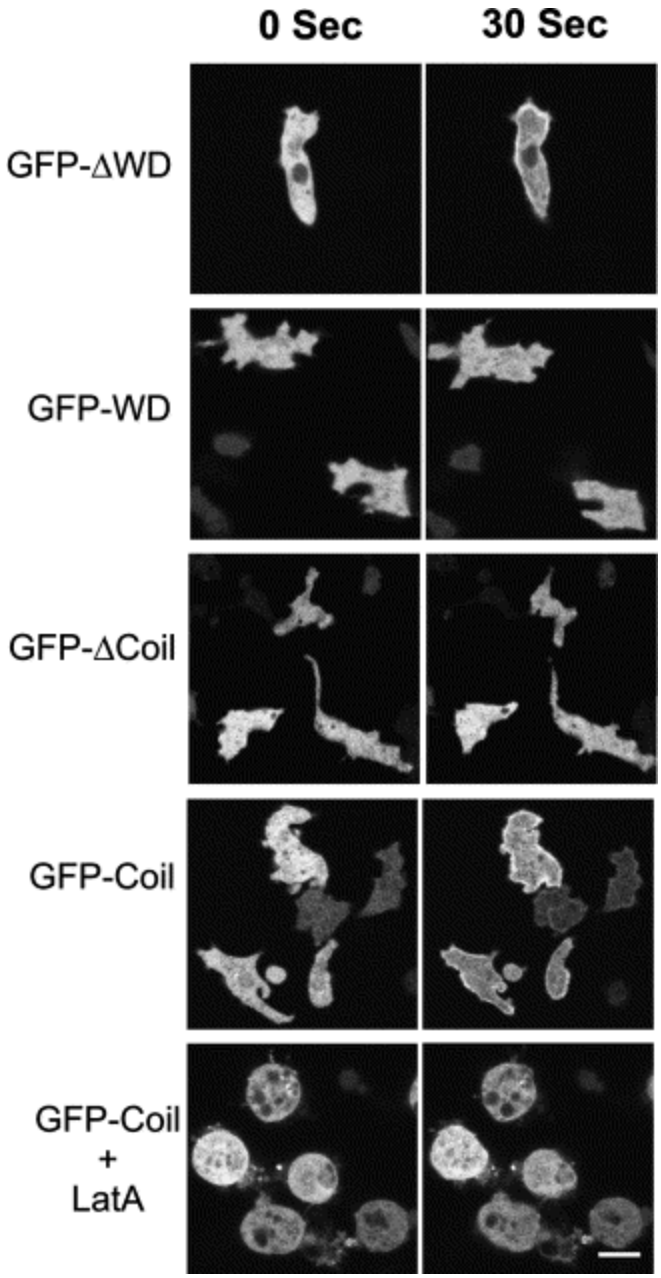

Fig. 2. Recruitment of GFP–MHCK A truncation constructs to the cell cortex in response to chemoattractant stimulation. Confocal microscope images were collected before (0 s) or after (30 s) stimulation with the chemoattractant cAMP. Bar, 10 μM.

To determine whether the coiled-coil domain could also mediate anterior localization observed for full-length MHCK A, we monitored localization during chemotactic migration. Cells migrating in chemotactic aggregation streams frequently displayed persistent enrichment of the GFP–Coil construct in anterior lamellipodial extensions, demonstrating that this domain is responsible for all the cellular localization behavior observed for full-length MHCK A (Fig. 3).

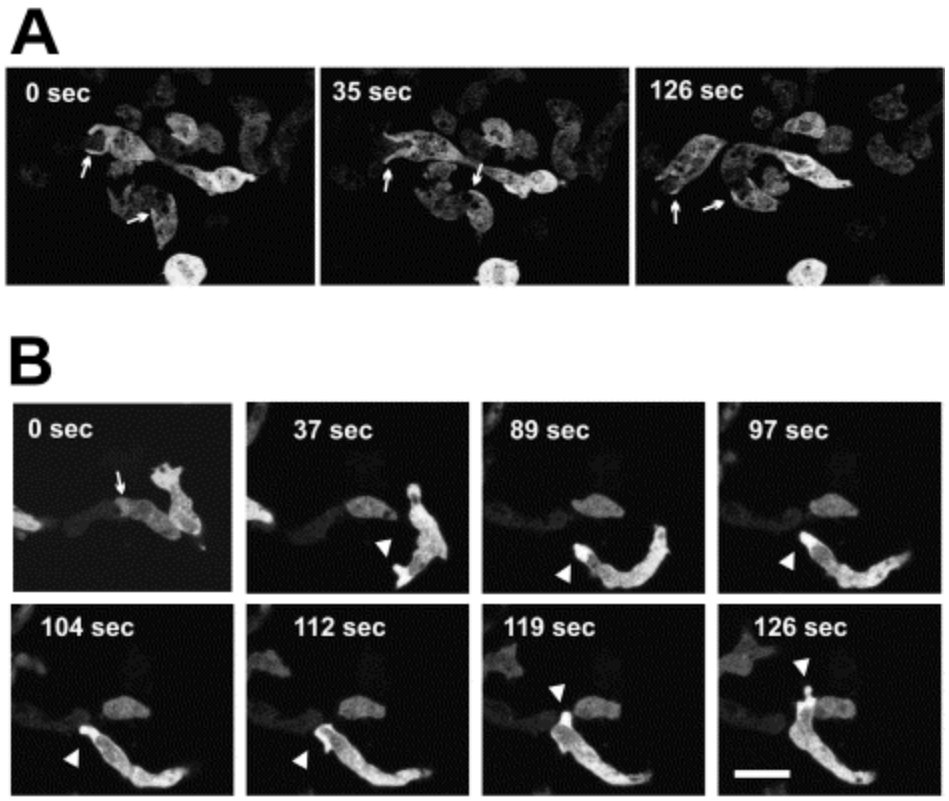

Fig. 3. Anterior localization of a GFP–Coil domain fusion protein during chemotactic cell migration. A: As with full-length GFP–MHCK A, cells that display anterior localization of GFP–Coil often do so persistently over several minutes. This series shows several cells engaged in apparent attempts to phagocytose cells ahead of them in streams. Arrows indicate anterior extensions that display enrichment of the GFP–Coil construct. The cell on the left eventually phagocytosed the cell ahead of it in the stream. B: This series shows one cell that displayed transient weak anterior enrichment of GFP–Coil (arrow), and another cell that displayed strong persistent anterior enrichment of the construct (arrowheads). Images collected by confocal microscopy at 7 s intervals. Bar, 20 μM.

One simple hypothesis for the dynamic localization behavior of MHCK A is that the protein contains sequences that confer F-actin binding. Database comparisons and sequence evaluation revealed no detectable similarity to known classes of actin-binding domains. However, in actin-binding tests with purified MHCK A, we observed co-sedimentation of full-length MHCK A with F-actin, with half-maximal binding of MHCK A occurring at approximately 4 μM F-actin (Fig. 4). To identify the F-actin-binding domain(s) of MHCK A we evaluated the co-sedimentation properties of a set of MHCK A truncation constructs in which either the WD repeat domain was removed (Δ-WD MHCK A) or in which the Coil domain was removed (Δ-Coil MHCK A). These constructs correspond to the truncations presented in Fig. 2, but contain amino-terminal 6× His tag fusions rather than GFP fusions. The Δ-WD MHCK A protein displayed co-sedimentation with F-actin similar to that of full-length MHCK A, while the Δ-Coil MHCK A protein displayed no co-sedimentation with F-actin (Fig. 5).

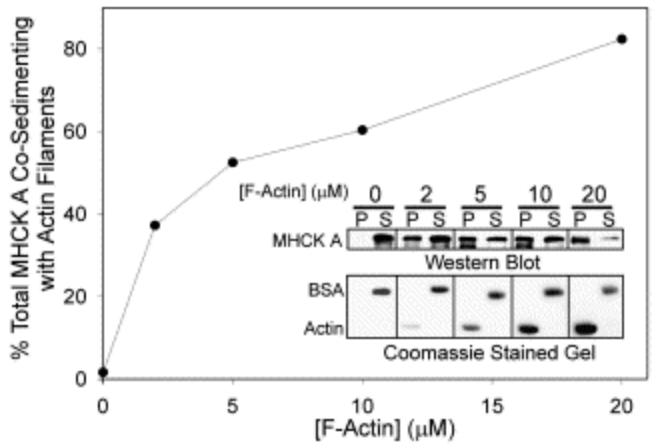

Fig. 4. Full-length MHCK A co-sediments with F-actin. Purified MHCK A (0.1 μM) was incubated with rabbit skeletal muscle F-actin at the indicated concentrations and subjected to ultracentrifugation as described in Section 2. Pellets and supernatants were evaluated by SDS–PAGE in conjunction with Western blots (to evaluate MHCK A abundance in pellets and supernatants) and Coomassie staining (to visualize F-actin and BSA).

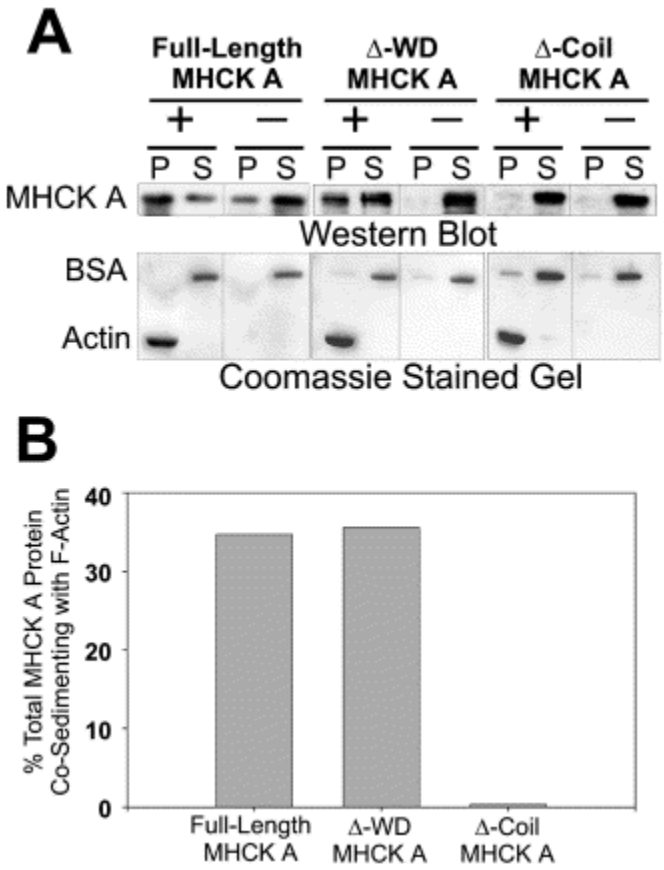

Fig. 5. Co-sedimentation of MHCK A truncation constructs with F-actin. Full-length and truncated constructs of MHCK A (0.1 μM) were incubated with 5.0 μM F-actin and the F-actin-binding activity was assessed as described in Section 2. Top panel as in Fig. 4. Bottom panel represents quantification of MHCK A co-sedimentation as determined via densitometry of Western blots of pellet and supernatant fractions.

4. Discussion

The results presented here indicate that MHCK A contains a previously unrecognized actin-binding activity within the coiled-coil domain of the protein. This F-actin-binding activity appears sufficient to explain the cellular translocation and anterior localization behavior displayed by native MHCK A. The strongest

enrichment of MHCK A is consistently to anterior actin-rich structures, as opposed to cortical actin in other regions of the cell. This may be due to the typically greater abundance and density of F-actin in pseudopodia and related structures, or this may reflect additional unidentified interactions that favor localization to these anterior structures.

MHCK A is one member of a group of related MHC kinases present in *Dictyostelium*. Gene disruption and cellular studies suggest that at least three members of this family (MHCK A, B, and C) have roles in the cellular localization of myosin [10] (and unpublished observations). MHCK B and C are both smaller enzymes that contain no detectable coiled-coil domain, and therefore might be predicted not to display the translocation behavior observed for MHCK A. We have recently found that MHCK C also displays dynamic recruitment to the cell cortex upon chemoattractant stimulation (unpublished observations). Since MHCK C lacks a coiled-coil domain, it is likely that cortical recruitment of this protein occurs by a distinct mechanism from that used by MHCK A, suggesting that these enzymes may be coupled to different signaling pathways or may have different cellular roles.

Earlier evaluation of MHCK A coiled-coil domain led to the prediction of a series of segments with very high probability of forming coiled-coil structure, with periodic breaks in the predicted coil structure [12]. Sequence analysis of this domain reveals no similarity to conserved classes of actin-binding domains such those of α-actinin, gelsolin, or ERM proteins. Although many established actin-binding proteins fall into classes related to the examples listed above, MHCK A and many other identified F-actin-binding proteins do not belong to conserved groups [24]. Tropomyosin represents one of the most extensively studied F-actin-binding proteins, and to our knowledge is also the only well-characterized actin-binding protein that consists mainly of a coiled-coil organization. Although the coiled-coil segment of MHCK A contains several short segments with low predicted coil probability [12], it appears possible that the MHCK A may represent another example of an actin-binding activity that operates by a mechanism related to that of tropomyosin. Further structural analysis of this domain will be important to address this possibility.

Acknowledgements
This work was supported by NIH Grant GM50009 to T.T.E., American Cancer Society Fellowship PF-99310-01-CSM to P.A.S., and CIHR Grant 8603 to G.P.C.

References
1. T.M. Svitkina, A.B. Verkhovsky, K.M. McQuade and G.G. Borisy *J. Cell Biol.* **139** (1997), pp. 397–415.
2. A.B. Verkhovsky, T.M. Svitkina and G.G. Borisy *J. Cell Biol.* **131** (1995), pp. 989–1002.
3. S. Yumura, H. Mori and Y. Fukui *J. Cell Biol.* **99** (1984), pp. 894–899.
4. P.Y. Jay, P.A. Pham, S.A. Wong and E.L. Elson *J. Cell Sci.* **108** (1995), pp. 387–393.
5. A.R. Horwitz and J.T. Parsons *Science* **286** (1999), pp. 1102–1103.
6. P.Y. Jay and E.L. Elson *Nature* **356** (1992), pp. 438–440.
7. J.P. Vaillancourt, C. Lyons and G.P. Côté *J. Biol. Chem.* **263** (1988), pp. 10082–10087.
8. D. Luck-Vielmetter, M. Schleicher, B. Grabatin, J. Wippler and G. Gerisch *FEBS Lett.* **269** (1990), pp. 239–243.
9. T.T. Egelhoff, R.J. Lee and J.A. Spudich *Cell* **75** (1993), pp. 363–371.
10. M.F. Kolman, L.M. Futey and T.T. Egelhoff *J. Cell Biol.* **132** (1996), pp. 101–109.
11. G.P. Côté, X. Luo, M.B. Murphy and T.T. Egelhoff *J. Biol. Chem.* **272** (1997), pp. 6846–6849.
12. L.M. Futey, Q.G. Medley, G.P. Côté and T.T. Egelhoff *J. Biol. Chem.* **270** (1995), pp. 523–529.
13. C.E. Clancy, M.G. Mendoza, T.V. Naismith, M.F. Kolman and T.T. Egelhoff *J. Biol. Chem.* **272** (1997), pp. 11812–11815.
14. X. Luo, S.W. Crawley, P.A. Steimle, T.T. Egelhoff and G.P. Côté *J. Biol. Chem.* **276** (2001), pp. 17836–17843.
15. A.G. Ryazanov, K.S. Pavur and M.V. Dorovkov *Curr. Biol.* **9** (1999), pp. R43–R45.

16. A.G. Ryazanov, M.D. Ward, C.E. Mendola, K.S. Pavur, M.V. Dorovkov, M. Wiedmann, H. Erdjument-Bromage, P. Tempst, T.G. Parmer, C.R. Prostko, F.J. Germino and W.N. Hait *Proc. Natl. Acad. Sci. USA* **94** (1997), pp. 4884–4889.
17. L.W. Runnels, L. Yue and D.E. Clapham *Science* **291** (2001), pp. 1043–1047.
18. P.A. Steimle, S. Yumura, G.P. Côté, Q.G. Medley, M.V. Polyakov, B. Leppert and T.T. Egelhoff *Curr. Biol.* **11** (2001), pp. 708–713.
19. S. Levi, M. Polyakov and T.T. Egelhoff *Plasmid* **44** (2000), pp. 231–238.
20. D. Knecht and K.M. Pang *Methods Mol. Biol.* **47** (1995), pp. 321–330.
21. M.F. Kolman and T.T. Egelhoff *J. Biol. Chem.* **272** (1997), pp. 16904–16910.
22. P.A. Steimle, T. Naismith, L. Licate and T.T. Egelhoff *J. Biol. Chem.* **276** (2001), pp. 6853–6860.
23. G.P. Côté and U. Bukiejko *J. Biol. Chem.* **262** (1987), pp. 1065–1072.
24. Pollard, T.D. 1999. In: Guidebook to the Cytoskeletal and Motor Proteins (Kreis, T. and Vale, R., Eds.), Oxford University Press, Oxford.